Inorg. Chem. **2006**, *45*, 8165–8174

Luminescent Phosphine Gold(I) Thiolates: Correlation between Crystal Structure and Photoluminescent Properties in $[R_3PAu\{SC(OMe)=NC_6H_4NO_2\text{-}4\}]$ (R = Et, Cy, Ph) and $[(Ph_2P\text{-}R\text{-}PPh_2)\{AuSC(OMe)=NC_6H_4NO_2\text{-}4\}_2]$ (R = CH_2, $(CH_2)_2$, $(CH_2)_3$, $(CH_2)_4$, Fc)

Soo Yei Ho,[†] Eddie Chung-Chin Cheng,[‡] Edward R. T. Tiekink,*[,§] and Vivian Wing-Wah Yam*[,‡]

Department of Chemistry, National University of Singapore, Singapore 117543, Centre for Carbon-Rich and Nano-Scale Metal-Based Materials Research and Department of Chemistry, The University of Hong Kong, Pokfulam Road, Hong Kong SAR, PR China, and The University of Texas, One UTSA Circle, San Antonio, Texas 78249-0698

Received May 14, 2006

X-ray crystallography shows the gold atoms in $[R_3PAu\{SC(OMe)=NC_6H_4NO_2\text{-}4\}]$ (R = Et, Cy, Ph; **1**–**3**, respectively) and $[(Ph_2P\text{-}R\text{-}PPh_2)\{AuSC(OMe)=NC_6H_4NO_2\text{-}4\}_2]$ (R = CH_2, $(CH_2)_2$, $(CH_2)_3$, $(CH_2)_4$, Fc; **4**–**8**, respectively) are linearly coordinated by phosphorus and thiolate-sulfur; weak intramolecular Au···O interactions are featured in all structures. The smaller ethyl substituents in **1** allow for supramolecular association via Au···S and Au···Au interactions that are not found in **2** and **3**, which contain larger phosphorus-bound Cy and Ph groups, respectively. Intramolecular Au···Au interactions are found in the dppm, dppe, dppp, and Fc structures but not in the dppp analogue, for which an anti conformation was found. The structures have been correlated with the results from photophysical study conducted in the solid state. Thus, photoexcitation of **1**–**7** with $\lambda > 350$ in the solid state and in solution produces green and blue luminescence, respectively. The spectra in each medium are remarkably similar to each other, and so the emission energy and excitation maxima observed for **1**–**7** appear to be independent of the nature of the ancillary phosphines, as well as the presence or absence of Au···Au interactions, either intermolecularly or intramolecularly.

Introduction

Gold and gold complexes exhibit a range of applications in contemporary society. Nanosized gold has generated enormous excitement in terms of catalytic applications,[1] and gold complexes have proven to be useful as drugs for the treatment of rheumatoid arthritis and bronchial asthma[2] and may be precursors for the gold plating of ceramics and electronic devices, as well as for gold thin films.[3] They also display interesting luminescence characteristics. While a range of gold complexes exhibit luminescence, such as gold thiolates,[4] nanosized gold,[5] anionic species,[6] oligomers[7] and

* To whom correspondence should be addressed. Phone: +1-210-458-5774. Fax: +1-210-458-7428. E-mail: edward.tiekink@utsa.edu (E.R.T.T.). Phone: +852-28592153. Fax: +852-28571586. E-mail: wwyam@hku.hk (V.W.-W.Y.).

[†] National University of Singapore.

[‡] The University of Hong Kong.

[§] The University of Texas.

(1) (a) Maye, M. M.; Luo, J.; Han, L.; Kariuki, N. N.; Zhong, C.-J. *Gold Bull.* **2003**, *36*, 75. (b) Corti, C. W.; Holliday, R. J.; Thompson, D. T. *Appl. Catal., A* **2005**, *291*, 253. (c) Maye, M. M.; Lim, I.-I. S.; Luo, J.; Rab, Z.; Rabinovich, D.; Liu, T.; Zhong, C.-J. *J. Am. Chem. Soc.* **2005**, *127*, 1519.

(2) Ho, S. Y.; Tiekink, E. R. T. In *Metallotherapeutic Drugs and Metal-Based Diagnostic Agents: The Use of Metals in Medicine*; Gielen, M., Tiekink, E. R. T., Eds.; John Wiley & Sons Ltd.: Chischester, U. K., 2005; Chapter 26, pp 507−527.

(3) (a) Aizenberg, J.; Black, A. J.; Whitesides, G. M. *Nature* **1998**, *394*, 868. (b) Schoenfisch, M. H.; Pemberton, J. E. *J. Am. Chem. Soc.* **1998**, *120*, 4502. (c) Aizenberg, J.; Black, A. J.; Whitesides, G. M. *J. Am. Chem. Soc.* **1999**, *121*, 4500. (d) Rapson, W. S.; Groenewald, T. In *Gold Usage*; Academic Press: London, 1978. (e) Okinaka, Y.; Hoshino, M. *Gold Bull.* **1998**, *31*, 3.

(4) Lee, Y.-A.; Eisenberg, R. *J. Am. Chem. Soc.* **2003**, *125*, 7778.

(5) Yamamoto, Y.; Shiotsuka, M.; Okuno, S.; Onaka, S. *Chem. Lett.* **2004**, *33*, 210.

(6) (a) Nicholson, P. G.; Ruiz, V.; Macpherson, J. V.; Unwin, P. R. *Chem. Commun.* **2005**, 1052. (b) Bouhelier, A.; Bachelot, R.; Lerondel, G.; Kostcheev, S.; Royer, P.; Wiederrecht, G. P. *Phys. Rev. Lett.* **2005**, *95*, 267405/1. (c) Yoshida, Y.; Fujii, J.; Saito, G.; Hiramatsu, T.; Sato, N. *J. Mater. Chem.* **2006**, *16*, 724.

10.1021/ic0608243 CCC: $33.50
Published on Web 09/08/2006

clusters,[8] organometallics,[8] oxo species,[10] and mixed-metal systems (e.g., with thallium[11] and silver),[12] phosphine gold(I) thiolates also demonstrate important luminescence characteristics.[13] Indeed, the formation of aurophilic interactions in solution has been used as a probe for detecting alkali metal ions.[14] Here, a dinuclear phosphine gold thiolate has been functionalized so that each thiolate ligand carries a macrocycle designed for specific coordination to K^+. When they encounter K^+, the macrocycles encapsulate the ion in a sandwich fashion, bringing the two gold atoms in close proximity which triggers luminescence because of the formation of an aurophilic (i.e., Au···Au) interaction. In addition to their role in luminescence, aurophilic interactions play an important role in the supramolecular aggregation patterns of gold compounds.

Gold complexes are known to exhibit a broad range of fascinating supramolecular architectures arising from, in addition to conventional intermolecular forces such as hydrogen bonding, the formation of the aforementioned aurophilic interactions.[15] Such aurophilic interactions are known to provide energy of stabilization to structures of the same order of magnitude as hydrogen-bonding interactions.[16] Hence, many supramolecular arrays can be thought of in terms of complementarity or competition between hydrogen-bonding interactions and aurophilic interactions, and this notion inspired the pioneering work of Schmidbaur.[16] Therefore, the structural chemistry of gold compounds attracts great attention that goes well beyond the determination of molecular structure and constantly reveals many highlights, such as the formation of luminescent hydrogen-bonded arrays,[17] and investigation of the influence of temperature dependence,[18] polymorphism, and phase transitions[19] upon luminescence.

In the present paper, the crystal structures of an unprecedented complete series of phosphine gold(I) thiolates (i.e., $[R_3PAu\{SC(OMe)=NC_6H_4NO_2\text{-}4\}]$, R = Et, Cy, Ph (**1**−**3**), and $[(Ph_2P\text{-}R\text{-}PPh_2)\{AuSC(OMe)=NC_6H_4NO_2\text{-}4\}_2]$, R = CH_2, $(CH_2)_2$, $(CH_2)_3$, $(CH_2)_4$, Fc (**4**−**8**)) are presented, where the thiolate ligand is derived from *O*-methyl-*N*-(4-nitrophenyl)thiocarbamide, $S=C(OMe)N(H)C_6H_4NO_2\text{-}4$.[20] Such a complete series allows for a systematic analysis of the principles dictating supramolecular aggregation in their crystal structures, as well as the correlation of their photoluminescent properties with the fine-tuning of the weak Au···Au interactions.

Metal complexes derived from related *O*-alkyl-*N*-arylthiocarbamides are known. Neutral forms of these ligands are known to coordinate gold[21] and palladium[22] via the thione sulfur atom. Usually, the ligand is found in the deprotonated form (i.e., as a carbonimidothioate) and has been shown to function as a thiolate ligand coordinating gold via the sulfur atom in $[Ph_3PAu\{SC(OMe)N=Ph\}]$,[23] related to the present report. More frequently, the anion coordinates as a S, N chelate as, for example, in complexes of rhenium[24] and technetium.[25] Bridging modes (i.e., μ_2 via sulfur and nitrogen[26] and μ_3 via bidentate sulfur and nitrogen)[27] have also been observed in some copper complexes.

Experimental Section

Materials. The chemicals and their sources used in the synthesis were sodium tetrachloroaurate(III) dihydrate (Aldrich), triethylphosphine gold(I) chloride (Strem), tricyclohexylphosphine (Fluka), triphenylphosphine (Fluka), bis(diphenylphosphino)methane (Al-

(7) (a) Mohamed, A. A.; Burini, A.; Fackler, J. P., Jr. *J. Am. Chem. Soc.* **2005**, *127*, 5012. (b). Hayashi, A.; Olmstead, M. M.; Attar, S.; Balch, A. L. *J. Am. Chem. Soc.* **2002**, *124*, 5791. (c) Lin, R.; Yip, J. H. K.; Zhang, K.; Koh, L. L.; Wong, K.-Y.; Ho, K. P. *J. Am. Chem. Soc.* **2004**, *126*, 15852. (d) Chui, S. S.-Y.; Chen, R.; Che, C.-M. *Angew. Chem.* **2006**, *45*, 1621.

(8) Chen, J.; Mohamed, A. A.; Abdou, H. E.; Krause Bauer, J. A.; Fackler, J. P., Jr.; Bruce, A. E.; Bruce, M. R. M. *Chem. Commun.* **2005**, 1575.

(9) (a) Li, P.; Ahrens, B.; Feeder, N.; Raithby, P. R.; Teat, S. J.; Khan, M. S. *Dalton Trans.* **2005**, 874. (b) Elbjeirami, O.; Omary, M. A.; Stender, M.; Balch, A. L. *Dalton Trans.* **2004**, 3173.

(10) Bojan, V. R.; Fernandez, E. J.; Laguna, A.; Lopez-de-Luzuriaga, J. M.; Monge, M.; Olmos, M. E.; Silvestru, C. *J. Am. Chem. Soc.* **2005**, *127*, 11564.

(11) Fernandez, E. J.; Laguna, A.; Lopez-de-Luzuriaga, J. M.; Elena O. M.; Perez, J. *Chem. Commun.* **2003**, 1760.

(12) (a) Catalano, V. J.; Moore, A. L. *Inorg. Chem.* **2005**, *44*, 6558. (b) Wang, Q.-M.; Lee, Y.-A.; Crespo, O.; Deaton, J.; Tang, C.; Gysling, H. J.; Gimeno, M. C.; Larraz, C.; Villacampa, M. D.; Laguna, A.; Eisenberg, R. *J. Am. Chem. Soc.* **2004**, *126*, 9488. (c) Colis, J. C. F.; Staples, R. J.; Tripp, C.; Labrecque, D.; Patterson, H. *J. Phys. Chem. B* **2005**, *109*, 102.

(13) (a) Assefa, Z.; McBurnett, B. G.; Staples, R. J.; Fackler, J. P., Jr.; Assmann, B.; Angermaier, K.; Schmidbaur, H. *Inorg. Chem.* **1995**, *34*, 75. (b) Hanna, S. D.; Khan, S. I.; Zink, J. I. *Inorg. Chem.* **1996**, *35*, 5813. (c) Yam, V. W.-W.; Chan, C.-L.; Cheung, K.-K. *J. Chem. Soc., Dalton Trans.* **1996**, 4019. (d) Tzeng, B.-C.; Chan, C.-K.; Cheung, K.-K.; Che, C.-M.; Peng, S.-M. *Chem. Commun.* **1997**, 135. (d) van Zyl, W. E.; Lopez-de-Luzuriaga, J. M.; Fackler, J. P., Jr. *J. Mol. Struct.* **2000**, *516*, 99. (e) Bardají, M.; Calhorda, M. J.; Costa, P. J.; Jones, P. G.; Laguna, A.; Reyes Pérez, M.; Villacampa, M. D. *Inorg. Chem.* **2006**, *45*, 1059. (f) Yun, S.-S.; Kim, J.-K.; Jung, J.-S.; Park, C.; Kang, J.-G.; Smyth, D. R.; Tiekink, E. R. T. *Cryst. Growth Des.* **2006**, *6*, 899.

(14) (a) Yam, V. W.-W.; Chan, C.-L.; Li, C.-K. *Angew. Chem., Int. Ed.* **1998**, *37*, 2857. (b) Li, C.-K.; Lu, X.-X.; Wong, K. M.-C.; Chan, C.-L.; Zhu, N.; Yam, V. W.-W. *Inorg. Chem.* **2004**, *43*, 7421. (c) Li, C.-K.; Cheng, E. C.-C.; Zhu, N.; Yam, V. W.-W. *Inorg. Chim. Acta* **2005**, *358*, 4191. (d) Yam, V. W.-W.; Cheng, E. C.-C. *Gold Bull.* **2001**, *34*, 20.

(15) (a) Mingos, D. M. P. *J. Chem. Soc., Dalton Trans.* **1976**, 1163. (b) Pyykkö, P. *Chem. Rev.* **1997**, *97*, 597. (c) Puddephatt, R. J. *Coord. Chem. Rev.* **2001**, *216*−*217*, 313.

(16) (a) Schneider, W.; Bauer, A.; Schmidbaur, H. *Organometallics* **1996**, *15*, 5445. (b) Tzeng, B.-C.; Schier, A.; Schmidbaur, H. *Inorg. Chem.* **1999**, *38*, 3978. (c) Schmidbaur, H. *Nature (London)* **2001**, *413*, 31.

(17) Paraschiv, C.; Ferlay, S.; Hosseini, M. W.; Bulach, V.; Planeix, J.-M. *Chem. Commun.* **2004**, 2270.

(18) Watase, S.; Kitamura, T.; Kanehisa, N.; Nakamoto, M.; Kai, Y.; Yanagida, S. *Chem. Lett.* **2003**, *32*, 1002.

(19) (a) White-Morris, R. L.; Olmstead, M. M.; Balch, A. L.; Elbjeirami, O.; Omary, M. A. *Inorg. Chem.* **2003**, *42*, 6741. (b) White-Morris, R. L.; Olmstead, M. M.; Balch, A. L. *J. Am. Chem. Soc.* **2003**, *125*, 1033. (c) Gussenhoven, E. M.; Fettinger, J. C.; Pham, D. M.; Malwitz, M. M.; Balch, A. L. *J. Am. Chem. Soc.* **2005**, *127*, 10838.

(20) Ho, S. Y.; Bettens, R. P. A.; Dakternieks, D.; Duthie, A.; Tiekink, E. R. T. *CrystEngComm* **2005**, *7*, 682.

(21) Bardi, R.; Del Pra, A.; Piazzesi, A.; M Sindellari, L.; Zarli, B. *Inorg. Chim. Acta* **1981**, *47*, 231.

(22) Casellato, U.; Fracasso, G.; Graziani, R.; Sindellari, L.; Sánchez González, A.; Nicolini, M. *Inorg. Chim. Acta* **1990**, *167*, 21.

(23) Hall, V. J.; Siasios, G.; Tiekink, E. R. T. *Aust. J. Chem.* **1993**, *46*, 561.

(24) Rossi, R.; Marchi, A.; Duatti, A.; Magon, L.; Cassellato, U.; Graziani, R. *J. Chem. Soc., Dalton Trans.* **1988**, 1857.

(25) Rossi, R.; Marchi, A.; Aggio, S.; Magon, L.; Duatti, A.; Cassellato, U.; Graziani, R. *J. Chem. Soc., Dalton Trans.* **1990**, 477.

(26) Abraham, S. P.; Narasimhamurthy, N.; Nethaji, M.; Samuelson, A. G. *Inorg. Chem.* **1993**, *32*, 1739.

(27) Narasimhamurthy, N.; Samuelson, A. G.; Manohar, H. *Chem. Commun.* **1989**, 1803.

drich), 1,2-bis(diphenylphosphino)ethane (Aldrich), 1,3-bis(diphenylphosphino)propane (Aldrich), 1,4-bis(diphenylphosphino)butane (Aldrich), 1,1′-bis(diphenylphosphino)ferrocene (Aldrich), thiodiglycol (Aldrich), and 4-nitrophenyl isothiocyanate (Lancaster). Dichloromethane, used in the photophysical measurements (LabScan), was purified and distilled in a nitrogen atmosphere using standard procedures prior to use. Methanol (Merck) and ethanol (Merck), used in photophysical measurements, were of GR grade, and all other solvents were of analytical grade and used without further purification.

Synthesis. The phosphine gold(I) chlorides, except for [Et_3PAuCl], were synthesized by the standard literature procedure (i.e., from the reduction of $HAuCl_4$ by thiodiglycol followed by the addition of the phosphine).[28] Similarly, the ligand employed in this study, S═C(OMe)N(H)$C_6H_4NO_2$-4, was prepared from the reaction of MeOH and 4-nitrophenyl isothiocyanate in accordance with the literature method.[20] The synthesis of the phosphine gold(I) thiolates was accomplished in quantitative yields using a metathetical reaction between the phosphine gold(I) chloride and the thiol in the presence of NaOH or KOH as described previously.[23] Crystals of **1**−**8** for the X-ray study were obtained in the same manner by layering ethanol on CH_2Cl_2 solutions of the complexes **1**−**7**, and in the case of **8**, the solvent combination was ether with $CHCl_3$.

Characterization and Spectroscopic Measurements. Infrared spectra for all compounds were recorded as KBr disks on a Bio-Rad FTS165 FTIR spectrophotometer. ^1H and $^{13}C\{^1H\}$ NMR spectra were recorded on a Bruker ACF300 FT NMR spectrometer operating at 300.145 and 75.479 MHz, respectively, with chemical shifts relative to tetramethylsilane. $^{31}P\{^1H\}$ NMR data were recorded on the same instrument operating at 121.442 MHz, but with the chemical shifts recorded relative to 85% aqueous H_3PO_4. Microanalyses were performed on a Perkin-Elmer PE 2400 CHN Elemental Analyzer. Melting points were determined on a Buchi Melting Point B-540 apparatus and were uncorrected. All electronic absorption spectra were recorded on a Hewlett-Packard 8452A diode-array spectrophotometer. Steady-state emission and excitation spectra recorded at room temperature and at 77 K were obtained on a Spex Fluorolog-3-211 fluorescence spectrophotometer with or without corning filters. All solutions for photophysical studies were prepared in a two-compartment cell consisting of a 10 cm^3 Pyrex bulb equipped with a sidearm to a 1 cm path length quartz cuvette and sealed from the atmosphere by a Rotaflo HP6/6 quick-release Teflon stopper. Solutions were degassed under high vacuum (limiting pressure < 10^{-3} Torr) with no less than four successive freeze−pump−thaw cycles. Solid-state photophysical measurements were carried out with solid samples loaded in a quartz tube inside a quartz-walled Dewar flask. Liquid nitrogen was placed into the Dewar flask for low-temperature (77 K) solid-state and glass photophysical measurements. Emission lifetime measurements were performed using a conventional laser system. The excitation source was the 355 nm output (third harmonic) of a Spectra-Physics Quanta-Ray Q-switched GCR-150-10 pulsed Nd:YAG laser. Luminescence decay signals were recorded on a Tektronix model TDS620A digital oscilloscope and analyzed using a program for exponential fits.

[Et_3PAu{SC(OMe)═$NC_6H_4NO_2$-4}] (1). mp: 87−89 °C. Anal. Calcd for $C_{14}H_{22}AuN_2O_3PS$: C, 32.20; H, 3.79; N, 5.33; S, 5.98. Found: C, 31.95; H, 4.21; N, 5.32; S, 6.09%. IR: ν(C−S) 1102m, 890m, ν(C−N) 1577s, ν(C−O) 1160m cm^{-1}. $^{31}P\{^1H\}$ NMR: δ 36.4.

[Cy_3PAu{SC(OMe)═$NC_6H_4NO_2$-4}] (2). mp: 152−154 °C. Anal. Calcd for $C_{26}H_{40}AuN_2O_3PS$: C, 45.35; H, 5.50; N, 4.10; S, 4.50. Found: C, 45.35; H, 5.85; N, 4.07; S, 4.66%. IR: ν(C−S) 1109m, 890m, ν(C−N) 1578s, ν(C−O) 1161m cm^{-1}. $^{31}P\{^1H\}$: δ 57.1.

[Ph_3PAu{SC(OMe)═$NC_6H_4NO_2$-4}] (3). mp: 146−147 °C. Anal. Calcd for $C_{26}H_{22}AuN_2O_3PS$: C, 46.76; H, 3.29; N, 4.25; S, 4.54. Found: C, 46.58; H, 3.31; N, 4.18; S, 4.78%. IR: ν(C−S) 1100m, 846m, ν(C−N) 1588s, ν(C−O) 1155m cm^{-1}. $^{31}P\{^1H\}$: 38.0.

[($Ph_2PCH_2PPh_2$){AuSC(OMe)═$NC_6H_4NO_2$-4}$_2$] (4). mp: 184 °C (dec). Anal. Calcd for $C_{41}H_{36}Au_2N_4O_6P_2S_2$: C, 40.91; H, 2.64; N, 4.70; S, 5.02. Found: C, 41.01; H, 3.02; N, 4.67; S, 5.34%. IR: ν(C−S) 1102m, 893m, ν(C−N) 1582s, ν(C−O) 1151m cm^{-1}. $^{31}P\{^1H\}$: δ 29.4.

[{$Ph_2P(CH_2)_2PPh_2$}{AuSC(OMe)═$NC_6H_4NO_2$-4)}$_2$] (5). mp: 167 °C (dec). Anal. Calcd for $C_{42}H_{38}Au_2N_4O_6P_2S_2$: C, 42.56; H, 2.97; N, 4.65; S, 5.08. Found: C, 42.53; H, 3.15; N, 4.61; S, 5.28%. IR: ν(C−S) 1100m, 892m, ν(C−N) 1577s, ν(C−O) 1150m cm^{-1}. $^{31}P\{^1H\}$: δ 35.7.

[{$Ph_2P(CH_2)_3PPh_2$}{AuSC(OMe)═$NC_6H_4NO_2$-4}$_2$] (6). mp: 155 °C (dec). Anal. Calcd for $C_{43}H_{40}Au_2N_4O_6P_2S_2$: C, 41.77; H, 3.17; N, 4.58; S, 4.92. Found: C, 42.03; H, 3.28; N, 4.56; S, 5.22%. IR: ν(C−S) 1100m, 892m, ν(C−N) 1580s, ν(C−O) 1150m cm^{-1}. $^{31}P\{^1H\}$: δ 30.9.

[{$Ph_2P(CH_2)_4PPh_2$}{AuSC(OMe)═$NC_6H_4NO_2$-4}$_2$] (7). mp: 170 °C (dec). Anal. Calcd for $C_{44}H_{42}Au_2N_4O_6P_2S_2$: C, 42.39; H, 3.35; N, 4.50; S, 4.87. Found: C, 42.52; H, 3.41; N, 4.51; S, 5.16%. IR: ν(C−S) 1105m, 891m, ν(C−N) 1576s, ν(C−O) 1160m cm^{-1}. $^{31}P\{^1H\}$: δ 33.9.

[($Ph_2PFcPPh_2$){AuSC(OMe)═$NC_6H_4NO_2$-4}$_2$] (8). mp: 163 °C (dec). Anal. Calcd for $C_{50}H_{42}Au_2FeN_4O_6P_2S_2$: C, 43.99; H, 3.20; N, 3.97; S, 4.27. Found: C, 43.81; H, 3.09; N, 4.09; S, 4.68%. IR: ν(C−S) 1100m, 847m, ν(C−N) 1571s, ν(C−O) 1168m cm^{-1}. $^{31}P\{^1H\}$: δ 32.2.

X-ray Crystallography. Intensity data were measured at 223(2) K on a Bruker SMART CCD diffractometer employing Mo Kα radiation so that θ_{max} was 30°. Data processing and empirical absorption correction were accomplished with the programs SAINT[29] and SADABS,[30] respectively. The structures were solved by heavy-atom methods,[31] and refinement (anisotropic displacement parameters, hydrogen atoms in the riding model approximation, and a weighting scheme of the form $w = 1/[\sigma^2(F_o^2) + aP^2 + bP]$ for $P = (F_o^2 + 2F_c^2)/3$) was on F^2.[32] In **1**, two positions were resolved for the C11−C12 residue, and from the refinement, the components were 0.60(1) and 0.40(1), respectively; only the major component is shown in Figure 1. Each of the C15−C21 cyclohexyl rings in **2** were found to be disordered over two positions. Each ring had a chair conformation but of a slightly different orientation. For the C15−C20 ring, the C16 and C20 atoms were common to both rings, and for the C15a−C20a ring, the C16 and C19 atoms were common; from the refinement, each disordered atom was assigned a site occupancy factor of 0.5. The rings were refined with the SAME command in SHELX[32] with soft constraints of C_1-C_2 = 1.54(1) Å and C_1-C_2 = 2.51(1) Å. Compound **8** was isolated as a

(28) Al-Saády, A. K.; McAuliffe, C. A.; Parish, R. V.; Sandbank, J. A. *Inorg. Synth.* **1985**, *23*, 191.
(29) *SAINT*, version 5.6; Bruker AXS Inc.: Madison, WI. 2000.
(30) (a) Sheldrick, G. M. *SADABS*; University of Göttingen: Göttingen, Germany, 2000. (b) Blessing, R. *Acta Crystallogr.* **1995**, A*51*, 33.
(31) Beurskens, P. T.; Admiraal, G.; Beurskens, G.; Bosman, W. P.; García-Granda, S.; Smits, J. M. M.; Smykalla, C. *The DIRDIF Program System*; Technical Report of the Crystallography Laboratory; University of Nijmegen: Nijmegen, The Netherlands, 1992.
(32) Sheldrick, G. M. *SHELXL97, Program for Crystal Structure Refinement*; University of Göttingen: Göttingen, Germany, 1997.

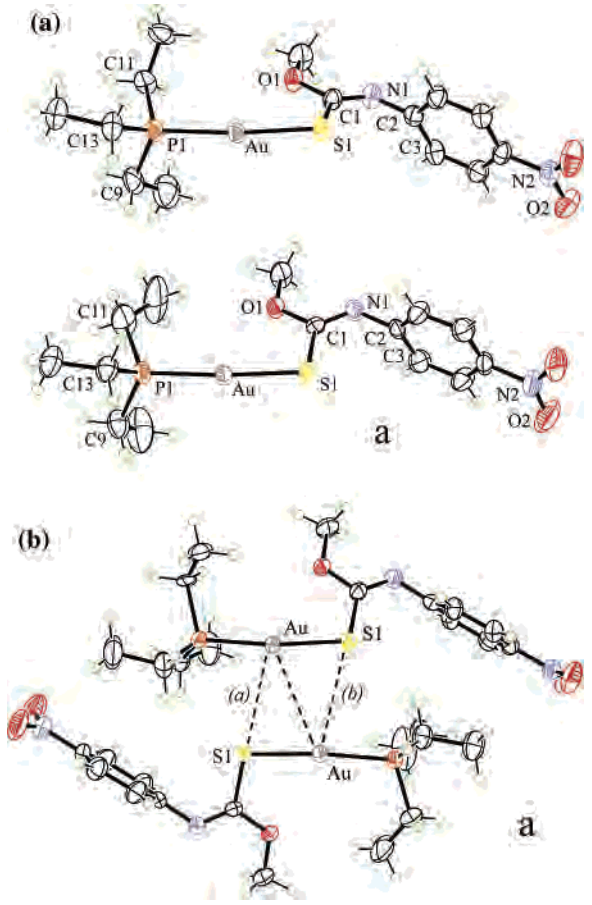

Figure 1. (a) Molecular structures for the two independent molecules of the asymmetric unit of [$Et_3PAu\{SC(OMe)=NC_6H_4NO_2\text{-}4\}$] (**1**); the atomic labels for the lower view have an "a" to distinguish this molecule from the upper view, see also Figures 2, 4, 5, and 7. (b) Supramolecular association in **1** via Au···S and Au···Au interactions.

dichloroform solvate. When significant, the largest residual electron density peaks in the refinements were in close vicinity to the gold atom. Crystallographic data and final refinement details are given in Table 1. Figures 1−8 were drawn with Ortep-3 for Windows[33] at the 50% probability level in each case. Data manipulation and interpretation were accomplished with teXsan[35] and PLATON,[34] respectively.

Results and Discussion

Synthesis and Characterization. The series of mononuclear complexes, [$R_3PAu\{SC(OMe)=NC_6H_4NO_2\text{-}4\}$], was prepared for R = Et (**1**), Cy (**2**), Ph (**3**), and the dinuclear complexes, [$(Ph_2PRPPh_2)\{AuSC(OMe)=NC_6H_4NO_2\text{-}4\}_2$], for R = CH_2 (**4**), $(CH_2)_2$ (**5**), $(CH_2)_3$ (**6**), $(CH_2)_4$ (**7**), and Fc (**8**) were synthesized in almost quantitative yields from the metathetical reaction between the phosphine gold(I) chloride and the sodium salt of the [$S=C(OMe)NC_6H_4NO_2\text{-}4$], generated in situ. The complexes are air and light stable and are soluble in common organic solvents. They have been characterized by elemental analysis and a range of spectroscopic methods. The ^1H NMR (see Supporting Information) exhibited the expected resonances and integration with the most notable feature being the absence of a broad resonance at 8.32 ppm, attributed to the N−H proton, that is evident in the spectrum of the ligand. Similarly, the $^{13}C\{^1H\}$ NMR (see Supporting Information) spectra show the expected resonances with the most prominent feature being the approximately 30 and 3 ppm upfield shifts in the resonances from the quarternary and methyl carbon atoms, respectively, upon coordination of the ligand. This observation is attributed to the substantial reorganization of π-electron density in the ligands because of the deprotonation and subsequent formation of a formal C=N double bond in the coordinated ligand. Both the mono- and binuclear complexes show a single resonance in their $^{31}P\{^1H\}$ NMR spectra with small (i.e., 1−5 ppm) downfield shifts compared with their precursor phosphine gold(I) chloride. The formation of a C=N double bond in the coordinated ligand is also indicated in the IR data because the absorptions attributed to ν(C−N) are shifted toward higher frequencies by over 100 wavenumbers; the broad absorption at 3236 cm^{-1} from ν(N−H) in the spectrum of free ligand is absent in those of the complexes. In addition to characteristic absorptions of ν(C−S) and ν(C−O), see the Experimental Section, antisymmetric and symmetric stretches of the NO_2 group are observed at ∼1377 and ∼1558 cm^{-1}, respectively.

Crystal and Molecular Structures. Full structural characterization of complexes **1**−**8** was afforded by single-crystal X-ray crystallography giving an unprecedented complete series of phosphine gold(I) thiolate structures. Selected geometric parameters for all structures are collected in Table 2. Two molecules of [$Et_3PAu\{SC(OMe)=NC_6H_4NO_2\text{-}4\}$] compose the asymmetric unit of **1**, as illustrated in Figure 1. Each gold atom exists in the expected linear geometry defined by a sulfur and phosphorus donor atom. The C1−S1 bond distances of 1.757(5) and 1.751(4) Å for the independent molecules have elongated significantly with respect to the comparable distance in the uncoordinated ligand (i.e., 1.664(2) Å), which has been reported to exist as a thione in the solid state and in its theoretical gas-phase structure.[20] This elongation is accompanied by a significant reduction in the C1−N1 bond distances to 1.262(5) and 1.264(5) Å (cf. 1.345(2) Å for the free ligand).[20] Clearly, these geometric parameters indicate that the ligand is functioning as a thiolate in coordination to gold. There is a marked variation in the angles about the C1 atom (Table 2). While the S1−C1−N1 angle is, as expected, ∼120°, the S1−C1−O1 angle is significantly contracted to 113° with a concomitant expansion of the S1−C1−N1 angle to approximately 126°. The reason for these distortions can be traced to the formation of an attractive Au···O interaction (i.e., Au···O1 are 2.957(3) and 2.968(3) Å for the independent molecules). These distances are within the sum of the van der Waals radii for gold and oxygen of 3.20 Å,[36] and while not representing significant bonding interactions, they are likely to be at least partly responsible for the deviation of the P−Au−S angles from the ideal l80°. Similar intramo-

(33) Farrugia, L. J. *J. Appl. Crystallogr.* **1997**, *30*, 565.
(34) *teXsan: Structure Analysis Software*; Molecular Structure Corp.: The Woodlands, TX, 1997.
(35) Spek, A. L. PLATON, A Multipurpose Crystallographic Tool; Utrecht, The Netherlands, 2006.
(36) Bondi, A. *J. Phys. Chem.* **1964**, *68*, 441.

Table 1. Crystallographic Parameters and Refinement Details for **1**−**8**

	1	**2**	**3**	**4**
formula	$C_{14}H_{22}AuN_2O_3PS$	$C_{26}H_{40}AuN_2O_3PS$	$C_{26}H_{22}AuN_2O_3PS$	$C_{41}H_{36}Au_2N_4O_6P_2S_2$
fw	526.33	688.60	670.45	1200.73
cryst syst	triclinic	triclinic	monoclinic	monoclinic
space group	$P\bar{1}$	$P\bar{1}$	$P2_1/c$	$C2/c$
a (Å)	11.3183(7)	9.8613(11)	9.1839(3)	27.9440(14)
b (Å)	13.7355(8)	11.7552(14)	16.0097(6)	10.8454(6)
c (Å)	14.4994(9)	25.971(3)	17.0530(6)	30.0702(15)
α (deg)	98.896(1)	97.21(1)	90	90
β (deg)	109.317(1)	100.37(1)	100.948(1)	115.497(1)
γ (deg)	114.323(1)	104.63(1)	90	90
V (Å^3)	1824.13(19)	2818.9(6)	2461.69(15)	8225.6(7)
Z	4	4	4	8
μ (cm^{-1})	8.279	5.378	6.157	7.358
D_x (g cm^{-3})	1.917	1.623	1.809	1.939
no. reflns	10 486	16 038	7121	11 974
no. obsd reflns with $I > 2\sigma(I)$	7705	9221	5811	7797
R (obsd data)	0.037	0.071	0.028	0.036
a and b in weighting scheme	0.028, 0	0.037, 8.234	0.021, 0	0.051, 0
R_w (all data)	0.079	0.200	0.061	0.112
CCDC no.	600356	600357	600358	600359

	5	**6**	**7**	**8**
formula	$C_{42}H_{38}Au_2N_4O_6P_2S_2$	$C_{43}H_{40}Au_2N_4O_6P_2S_2$	$C_{44}H_{42}Au_2N_4O_6P_2S_2$	$C_{50}H_{42}Au_2FeN_4O_6P_2S_2{\cdot}2CHCl_3$
fw	1214.76	1228.78	1242.81	1609.45
cryst syst	monoclinic	orthorhombic	monoclinic	monoclinic
space group	$P2_1/c$	$Pbcn$	$P2/n$	$C2/c$
a (Å)	11.9428(5)	19.077(3)	22.3284(7)	23.1341(11)
b (Å)	31.5866(13)	8.5623(13)	8.5861(3)	12.1157(6)
c (Å)	11.6265(5)	26.017(4)	23.9840(7)	21.9265(10)
α (deg)	90	90	90	90
β (deg)	106.658(1)	90	98.111(1)	109.478(1)
γ (deg)	90	90	90	90
V (Å^3)	4201.8(3)	4249.8(11)	4552.1(3)	5794.0(5)
Z	4	4	4	4
μ (cm^{-1})	7.203	7.123	6.651	5.754
D_x (g cm^{-3})	1.920	1.921	1.813	1.845
no. reflns	12169	6147	13160	8396
no. obsd reflns with $I > 2\sigma(I)$	9054	4228	7526	6594
R (obsd data)	0.046	0.044	0.055	0.031
a and b in weighting scheme	0.023, 0	0.051, 0	0.042, 8.192	0.045, 0
R_w (all data)	0.083	0.111	0.126	0.087
CCDC no.	600360	600361	600362	600363

lecular Au···O interactions have been noted previously in structural phosphine gold thiolate chemistry.[37] The major differences between the two independent molecules of **1** in the asymmetric unit are conformational and are reflected in the torsion angle data collected in Table 2. These data indicate that the Au/S1/C1/O1/N1 portion of the thiolate ligand is essentially planar but that this planarity does not extend to the aromatic ring. In addition, as evident in Figure 1, there is a significant twist about the P1−C11 bond resulting in a different relative orientation of this ethyl substituent; the respective Au/P1/C11/C12 torsion angles are −60.2(9) and 23.9(8)°. In the crystal structure of **1**, the independent molecules associate about a pseudocenter of inversion to form a dimeric pair mediated by Au···Au and Au···S interactions. The Au···Au separation is 3.6086(4) Å, and in reference to the labels in Figure 2, the Au···S separations are shorter at 3.4648(14) (a) and 3.5384(14) Å (b); the sum of the van der Waals radii for gold and sulfur is 4.0 Å.[36] Increasing the size of the phosphorus-bound R groups, to Cy (**2**) and Ph (**3**), precludes such intermolecular associations.

Two independent molecules compose the asymmetric unit of **2**. As shown in Figure 2 and from the torsion angle data collected in Table 2, there are conformational differences between them with respect to the relative orientations of the cyclohexyl rings. In terms of geometric parameters, they match closely those found in **1**. The same is true for the R = Ph analogue (**3**), Figure 3, and indeed for subsequent structures, and so these are not discussed further in any detail. Consistent with the increased size of the Cy and Ph groups, the intramolecular Au···O distances are elongated with respect to the situation in **1**. The remaining structures to be described are dinuclear gold species.

The dppm ligand in $(Ph_2P(CH_2)PPh_2)\{Au[SC(OMe)=NC_6H_4NO_2\text{-}4]\}_2$ (**4**) (Figure 4a) adopts a syn conformation allowing for the formation of an intramolecular Au···Au interaction of 3.1589(4) Å. This interaction in effect clips the two halves of the molecule into an "A-frame" conformation, as seen in the torsion angle defined by P1/Au1/Au1a/P1a of 23.60(6)°. The dimers of **4** further associate with a centrosymmetrically related dimer (−x, −y, −z) to form the

(37) Siasios, G.; Tiekink, E. R. T. *Z. Kristallogr.* **1993**, *204*, 95. (b) Siasios, G.; Tiekink, E. R. T. *Z. Kristallogr.* **1993**, *205*, 261. (c) Römbke, P.; Schier, A.; Schmidbaur, H. *J. Chem. Soc., Dalton Trans.* **2001**, 2482.

Table 2. Crystallographic Parameters (Å, deg) for **1**−**8**

	1	**1a**	**2**	**2a**	**3**	**4**	**4a**
Au−S1	2.3059(11)	2.3165(11)	2.306(2)	2.301(2)	2.3119(7)	2.3103(15)	2.3023(14)
Au−P1	2.2510(13)	2.2601(12)	2.269(2)	2.266(2)	2.2573(7)	2.2651(14)	2.2522(14)
S1−C1	1.757(5)	1.751(4)	1.744(9)	1.748(11)	1.754(3)	1.751(6)	1.763(6)
O1−C1	1.346(5)	1.344(5)	1.353(11)	1.351(11)	1.354(3)	1.346(7)	1.349(7)
N1−C1	1.262(5)	1.264(5)	1.276(12)	1.253(13)	1.267(4)	1.266(7)	1.259(7)
N1−C2	1.389(6)	1.406(6)	1.406(12)	1.411(12)	1.401(4)	1.402(8)	1.422(8)
Au···O	2.957(3)	2.968(3)	3.066(6)	3.172(8)	2.989(2)	3.082(5)	2.963(5)
S1−Au−P1	172.61(5)	174.77(4)	174.71(8)	171.89(11)	177.47(3)	174.56(6)	173.67(5)
Au−S1−C1	101.27(16)	102.44(15)	104.9(3)	107.5(3)	103.29(10)	103.8(2)	101.9(2)
S1−C1−O1	113.3(3)	113.4(3)	114.5(6)	114.4(8)	112.98(19)	114.8(4)	113.6(4)
S1−C1−N1	126.5(4)	126.1(4)	124.6(8)	125.2(8)	127.0(2)	126.0(5)	126.0(5)
O1−C1−N1	120.2(4)	120.5(4)	120.9(8)	120.5(10)	119.9(3)	119.2(5)	120.4(6)
C1−O1−C8	116.3(4)	116.0(4)	116.4(8)	114.3(8)	116.6(2)	115.5(5)	114.9(5)
C1−N1−C2	121.7(4)	120.6(4)	118.4(8)	120.5(9)	121.9(3)	122.5(6)	120.3(6)
Au−S1−C1−O1	14.6(5)	−2.0(4)	3.5(8)	13.1(9)	−3.0(2)	−16.7(5)	−6.4(5)
Au−S1−C1−N1	−165.8(5)	178.2(5)	−179.0(8)	−167.0(10)	−179.6(3)	165.1(5)	174.6(6)
S1−C1−N1−C2	−1.2(9)	−0.5(8)	3.9(14)	1.0(17)	−2.0(4)	−2.5(9)	−2.5(10)
P1−Au−S1−C1	−10.6(6)	2.8(7)	157.7(10)	152.8(7)	17.4(7)	−34.8(8)	55.7(6)
C1−N1−C2−C3	116.2(6)	99.2(7)	82.5(13)	−85.1(15)	−69.2(4)	−103.1(8)	−96.1(9)

	5	**5a**	**6**	**7**	**7a**	**8**
Au−S1	2.3102(13)	2.3105(14)	2.3255(15)	2.3032(19)	2.2975(19)	2.3274(9)
Au−P1	2.2568(13)	2.2662(14)	2.2679(15)	2.2418(16)	2.2449(15)	2.2651(9)
S1−C1	1.744(6)	1.747(6)	1.758(6)	1.749(7)	1.759(8)	1.747(4)
O1−C1	1.358(6)	1.355(6)	1.375(7)	1.352(8)	1.358(8)	1.356(4)
N1−C1	1.276(6)	1.261(7)	1.248(7)	1.257(8)	1.261(8)	1.260(5)
N1−C2	1.397(7)	1.406(7)	1.402(8)	1.406(8)	1.390(8)	1.397(5)
Au···O	3.049(4)	3.086(4)	2.938(4)	2.982(5)	2.975(5)	3.102(3)
S1−Au−P1	177.78(5)	172.36(5)	172.29(5)	176.62(6)	176.98(9)	174.73(4)
Au−S1−C1	103.31(18)	105.4(2)	101.8(2)	102.6(3)	103.1(2)	105.63(13)
S1−C1−O1	115.1(4)	114.3(4)	112.4(4)	113.1(5)	112.5(5)	114.0(3)
S1−C1−N1	125.6(4)	127.3(5)	128.1(5)	125.1(5)	126.5(6)	126.3(3)
O1−C1−N1	119.3(5)	118.4(5)	119.5(6)	121.8(6)	121.1(7)	119.7(3)
C1−O1−C8	115.9(4)	114.9(4)	115.1(5)	117.2(6)	115.7(6)	115.0(3)
C1−N1−C2	120.7(5)	125.2(5)	125.0(5)	119.4(6)	122.2(6)	121.7(4)
Au−S1−C1−O1	12.4(4)	−5.5(5)	−2.0(5)	−13.1(5)	−8.2(5)	8.1(3)
Au−S1−C1−N1	−168.1(5)	172.3(5)	178.0(5)	169.6(6)	171.4(6)	−172.4(4)
S1−C1−N1−C2	1.6(8)	−4.1(9)	−1.2(10)	−4.9(10)	4.4(10)	1.9(6)
P1−Au−S1−C1	9.9(14)	−115.2(4)	6.6(5)	−4.2(13)	−95.7(15)	93.3(4)
C1−N1−C2−C3	−110.6(6)	67.0(8)	−91.7(8)	110.0(8)	−126.9(8)	91.4(6)

tetrameric unit shown in the lower view of Figure 4b. The primary contacts between the dimers are provided by Au···S interactions so that Au···$S1_i$ is 3.6978(18) Å. The dinuclear structure of [($Ph_2PCH_2PPh_2$){AuSC(OMe)=NC_6H_4-NO_2-4}$_2$] (**5**) (Figure 5) adopts a somewhat twisted A-frame conformation, with P1/Au1/Au1a/P1a being 52.87(5)°, and it also features an intramolecular Au···Au interaction that is shorter (i.e., 3.1171(3) Å) than that observed in **4**. An even shorter intramolecular Au···Au interaction of 3.0820(6) Å is found in the dppp analogue (**6**) (Figure 6). The molecule has crystallographically imposed 2-fold symmetry (−*x*, *y*, 1/2 − *z*), and the twist in the molecule, as reflected in the $P1/Au1/Au^i/P^i$ torsion angle of 72.28(6)° suggests the dppm-, dppe-, and dppp-containing molecules contort to maximize the Au···Au interactions. An entirely different conformation is found in the dppb analogue (**7**) (Figure 7), for which an anti conformation is found. It is likely that, for the shorter $(CH_2)_n$ bridges between the phosphorus atoms, the Au···Au interactions are able to stabilize the syn conformation, but beyond the $n = 3$ threshold, intramolecular Au···Au interactions are not found. Indeed, all of the known [{$Ph_2P(CH_2)_2$-PPh_2}{Au(SR)}$_2$] structures[38−41] feature a similar anti conformation, and only in two structures are intermolecular Au···Au interactions found.[38,41] It is clear that, generally, syn conformations are rare in dppb complexes involving gold, with the notable exception being found in the structure of [{$Ph_2P(CH_2)_4PPh_2$}$(AuCl)_2$], in which an approximate syn arrangement is stabilized by intermolecular Au···Cl interactions provided by a solvent dichloromethane molecule.[42] In the case of **7**, it is likely that intermolecular aurophilic interactions are precluded because of the size of the thiolate ligand combined with the presence of the intramolecular Au···O interactions that serve to reduce the residual Lewis

(38) Narayanaswamy, R.; Young, M. A.; Parkhurst, E.; Ouellette, M.; Kerr, M. E.; Ho, D. M.; Elder, R. C.; Bruce, A. E.; Bruce, M. R. M. *Inorg. Chem.* **1993**, *32*, 2506.
(39) Tzeng, B.-C.; Zank, J.; Schier, A.; Schmidbaur, H. *Z. Naturforsch. B* **1999**, *54*, 825.
(40) Maspero, A.; Kani, I.; Mohamed, A. A.; Omary, M. A.; Staples, R. J.; Fackler, J. P., Jr. *Inorg. Chem.* **2003**, *42*, 5311.
(41) Onaka, S.; Yaguchi, M.; Yamauchi, R.; Ozeki, T.; Ito, M.; Sunahara, T.; Sugiura, Y.; Shiotsuka, M.; Nunokawa, K.; Horibe, M.; Okazaki, K.; Iida, A.; Chiba, H.; Inoue, K.; Imai, H.; Sako, K. *J. Organomet. Chem.* **2005**, *690*, 57.
(42) Schmidbaur, H.; Bissinger, P.; Lachmann, J.; Steigelmann, O. *Z. Naturforsch. B* **1992**, *47*, 1711.

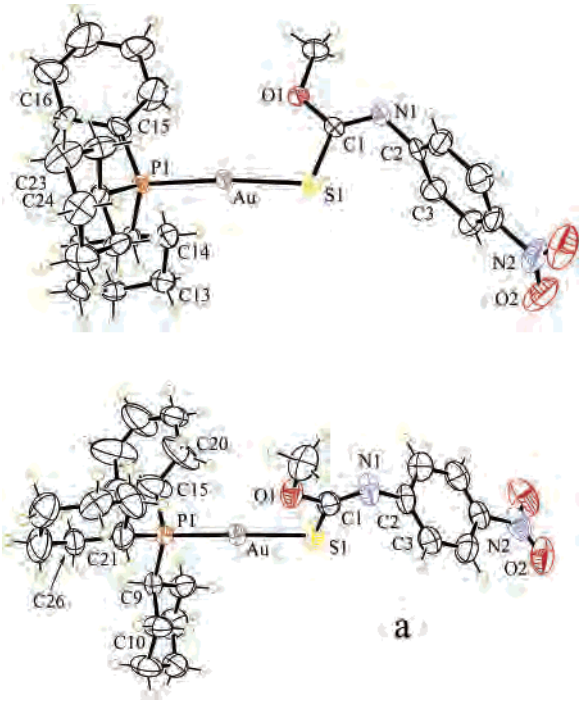

Figure 2. Molecular structures for the two independent molecules of the asymmetric unit of [$Cy_3PAu\{SC(OMe)=NC_6H_4NO_2\text{-}4\}$] (**2**). For each molecule, only one component of the disordered C15−C20 ring is shown for clarity.

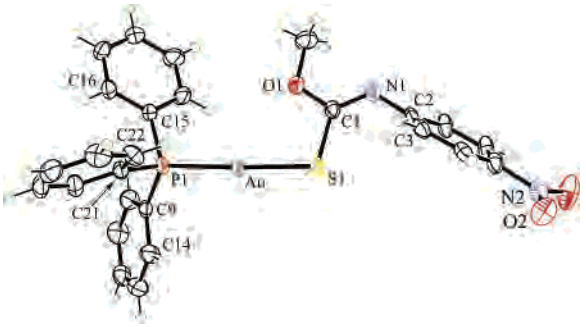

Figure 3. Molecular structure of [$Ph_3PAu\{SC(OMe)=NC_6H_4NO_2\text{-}4\}$] (**3**).

acidity of the gold centers. The final structure to be described is that of the Fc analogue, [$\{Ph_2P(Fc)PPh_2\}\{AuSC(OMe)=NC_6H_4NO_2\text{-}4\}_2$] (**8**). The molecule (Figure 8) has crystallographic 2-fold symmetry ($-x$, y, $1/2 - z$) and features an intermolecular Au···Au interaction of 2.9765(3) Å (i.e., the shortest among the structures described herein). The P1/Au/Au^i/P1^i torsion angle is 85.12(3)°, reinforcing the trend between shorter Au···Au interactions and the orthogonal P/Au/Au/P relationship. The P1/Cg1/Cg1^i/P1^i angle is 55.39(5)°, where Cg1 is the ring centroid of the Cp ring, and this indicates a conformation of the Fc group between synclinal staggered (36°) and synclinal eclipsed (72°); the Fe···Cg1 distance is 1.642(2) Å.[43] Complex **8** was characterized as its chloroform solvate so that, for each dinuclear species, there are two chloroform molecules. The solvent molecules associate with the complex via a C26−H···S1^{ii} interaction so that H···S^{ii} is 2.75 Å, C26···S1^{ii} is 3.533(7) Å, and the angle at H is 137° (for ii $-x$, $-1 + y$, $1/2 - z$).

(43) Bandoli, G.; Dolmella, A. *Coord. Chem. Rev.* **2000**, *209*, 161.

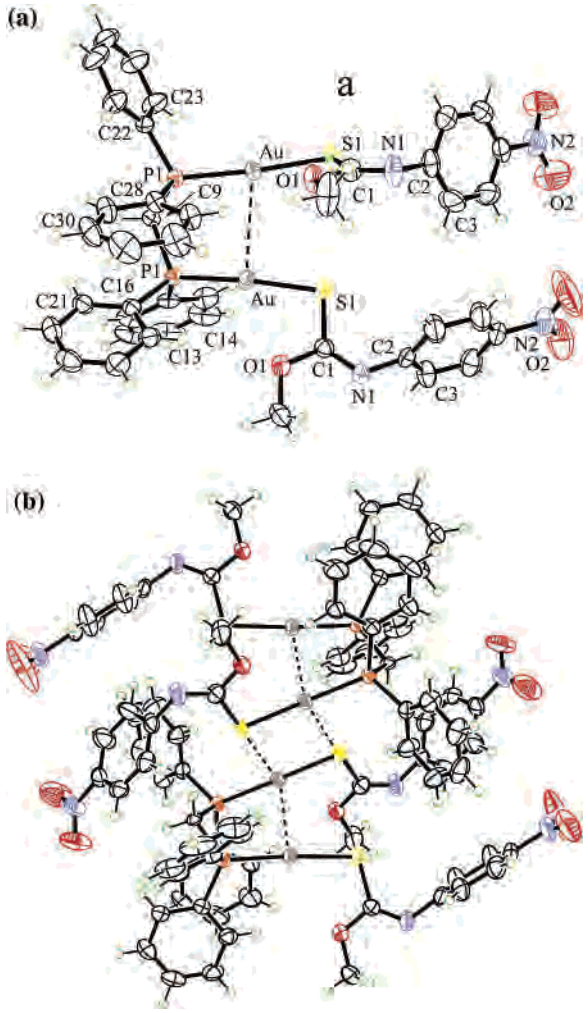

Figure 4. (a) Molecular structure of [$(Ph_2PCH_2PPh_2)\{AuSC(OMe)=NC_6H_4NO_2\text{-}4\}_2$] (**4**). (b) Supramolecular association in **4** via Au···S interactions to form a tetramer.

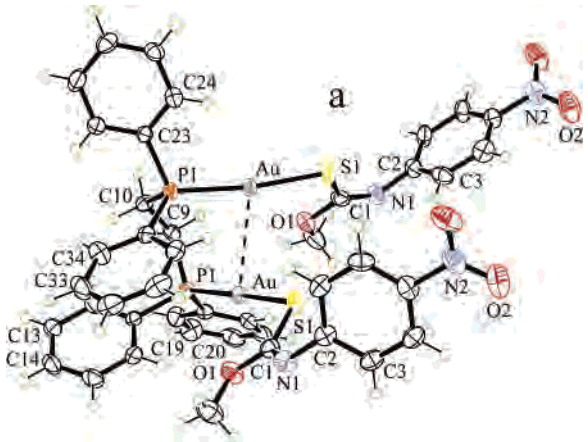

Figure 5. Molecular structure of [$(Ph_2P(CH_2)_2PPh_2)\{AuSC(OMe)=NC_6H_4NO_2\text{-}4\}_2$] (**5**).

The availability of the complete "set" of structures, **1**−**8**, allows a few general conclusions to be made.

First and foremost, there is no significant influence exerted by the nature of the phosphine ligand in **1**−**8** on the mode of coordination of the thiolate ligand. Thus, the geometric parameters within the thiolate ligand are experimentally equivalent throughout the entire series. In the same way, in

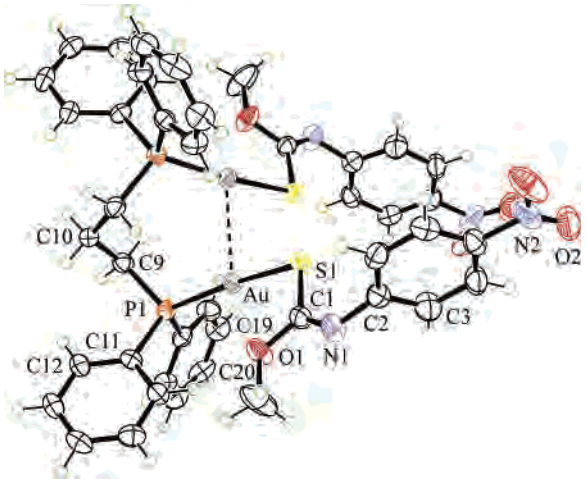

Figure 6. Molecular structure of [{$Ph_2P(CH_2)_3PPh_2$}{AuSC(OMe)═$NC_6H_4NO_2$-4}$_2$] (**6**).

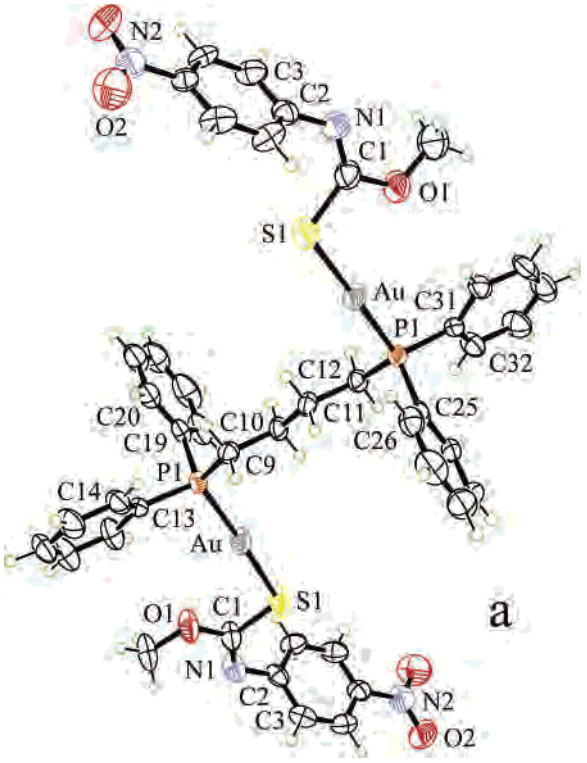

Figure 7. Molecular structure of [{$Ph_2P(CH_2)_4PPh_2$}{AuSC(OMe)═$NC_6H_4NO_2$-4}$_2$] (**7**).

terms of the gold atom, the Au−S distances lie in the narrow range from 2.2975(19) (for **7a**) to 2.3274(9) Å (**8**) (i.e., encompassing structures with and without, respectively, Au···Au interactions); the R = Et structure, with a close Au···Au interaction, has an experimentally equivalent Au−S distance of 2.3059(11) Å to that observed in **7a**, without a significant Au···Au contact. The Au−P distances lie within an even narrower range from 2.2418(16) (**7**) to 2.269(2) Å (**2**). A common feature of all eight structures is the planarity of the S1/O1/N1/C1 chromophore and its conformation with respect to the gold atom, as well as the orientation of the nitrogen-bound aromatic ring to the central chromophore, as reflected in the C1/N1/C2/C3 torsion angle data. Conformational differences in the structures occur in the relative

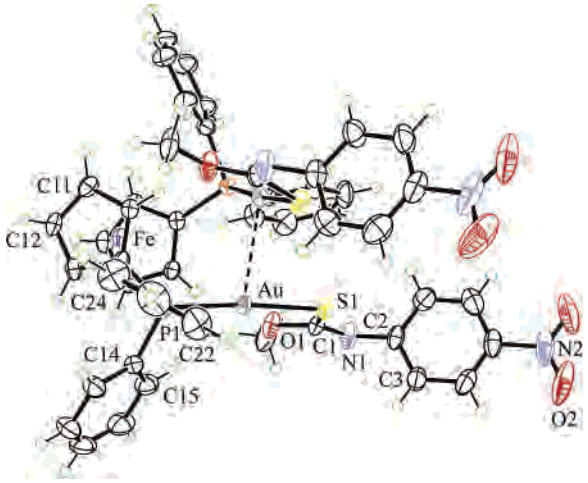

Figure 8. Molecular structure of [{$Ph_2P(Fc)PPh_2$}{AuSC(OMe)═NC_6H_4-NO_2-4}$_2$] (**8**).

disposition of the thiolate ligand to the P1−Au−S1 vector (i.e., the P1/Au/S1/C1 torsion angles vary from coplanarity (e.g., 3° in **1a**) to orthogonal (e.g., 87° in **8**)). In terms of supramolecular aggregation, in the mononuclear complexes, Au···Au and Au···S interactions are found in **1** but are absent in **2** and **3**, an observation that can be readily correlated with the presence of the large phosphorus-bound R groups in the latter that preclude the close approach of the molecules.[44] Significant twisting in the dinuclear structures, [{$Ph_2P(CH_2)_n$-PPh_2}{AuSC(OMe)═$NC_6H_4NO_2$-4}$_2$], n = 1−3, and [{Ph_2P-(Fc)PPh_2}{AuSC(OMe)═$NC_6H_4NO_2$-4}$_2$], as shown in the P1/Au/Au′/P1′ torsion angle data, allows for the formation of intramolecular Au···Au interactions so that the Au···Au contacts vary from a long 3.1589(4) Å in **4** to 2.9765(3) Å in **8**. Steric constraints preclude the formation of both intra- and intermolecular Au···Au interactions in the case of the n = 4 complex, **7**. Having established the crystal and molecular structures of **1**−**8**, we thought it would be of significant interest to determine the luminescence characteristics of these complexes in the solid state to establish relationships between the adopted structure, in particular, the presence of Au···Au interactions or otherwise and photoluminescence.

Photophysical Behavior. The electronic absorption data of complexes **1**−**8** in dichloromethane are tabulated in Table 3. In general, they are dominated by a number of ill-defined high-energy absorption shoulders at ∼260−262, 266−270, and 274−298 nm and a low-energy absorption band at ∼330−334 nm. An additional absorption tail beyond 420 nm is also observed for **8**. The electronic absorption spectra of **4** and **8** in dichloromethane at 298 K are shown in Figure 9 as selected examples. By comparison with the absorption data of the ligand and those of related gold(I) phosphine systems,[13c,14] the shoulders at ∼260−262 nm can readily be attributed to the a carbonimidothioate ligand-centered $\pi-\pi^*$ transition since the ligand itself also exhibits a similar shoulder at ∼256 nm. The absorption shoulder at ∼266−270 nm observed for complexes **2** and **4**−**8** is assigned as

(44) Smyth, D. R.; Vincent, B. R.; Tiekink, E. R. T. *Z. Kristallogr.* **2001**, *216*, 298.

Table 3. Photophysical Data for the Ligand, [S=C(OMe)N(H)$C_6H_4NO_2$-4], and Complexes **1**−**8**

compound	abs in CH_2Cl_2 λ_{abs} (nm) (ϵ ($M^{-1}cm^{-1}$))	medium (T (K))	emission λ_{em} (nm) (τ_0 (ms))
ligand		solid (298)	nonemissive
	256 sh (7000),	solid (77)	535 (0.0057)
	330 (17 450)	glass (77)[a]	510 (5.72, 59.22)[b]
		CH_2Cl_2 (298)	nonemissive
1		solid (298)	481[c]
	334 (13 550)	solid (77)	538 (5.14)
		glass (77)[a]	523 (4.46)
		CH_2Cl_2 (298)	486[c]
2		solid (298)	482[c]
	260 sh (8300),	solid (77)	526 (3.26)
	298 sh (9750),	glass (77)[a]	521 (6.02)
	332 (16 000)	CH_2Cl_2 (298)	488[c]
3	260 sh (9350),	solid (298)	nonemissive
	268 sh (8200),	solid (77)	517 (2.28)
	276 sh (7100),	glass (77)[a]	518 (3.90)
	332 (14 200)	CH_2Cl_2 (298)	481[c]
4	260 sh (28 950),	solid (298)	510[c]
	270 sh (26 800),	solid (77)	541 (2.21)
	276 sh (24 050),	glass (77)[a]	529 (4.70)
	332 (30 100)	CH_2Cl_2 (298)	488[c]
5	260 sh (18 600),	solid (298)	471 (0.0050)
	266 sh (17 350),	solid (77)	541 (3.90)
	276 (15 350),	glass (77)[a]	530 (0.73,3.96)[b]
	332 (29 650)	CH_2Cl_2 (298)	482[c]
6		solid (298)	491 (0.0048)
	268 sh (15 500),	solid (77)	543 (4.73)
	276 sh (13 100),	glass (77)[a]	518 (3.86)
	332 (29 650)	CH_2Cl_2 (298)	482[c]
7	260 sh (16 200),	solid (298)	500 (0.0053)
	268 sh (14 450),	solid (77)	537 (2.60)
	274 (12 600),	glass (77)[a]	538 (3.15)
	332 (28 750)	CH_2Cl_2 (298)	484[c]
8		solid (298)	nonemissive
	262 sh (27 150),	solid (77)	nonemissive
	274 sh (21 050),	glass (77)[a]	506[c]
	332 (31 650)	CH_2Cl_2 (298)	nonemissive

[a] In EtOH−MeOH−CH_2Cl_2 4:1:1 (v/v) at 77 K. [b] Double exponential decay. [c] Luminescence lifetime shorter than 0.1 μs.

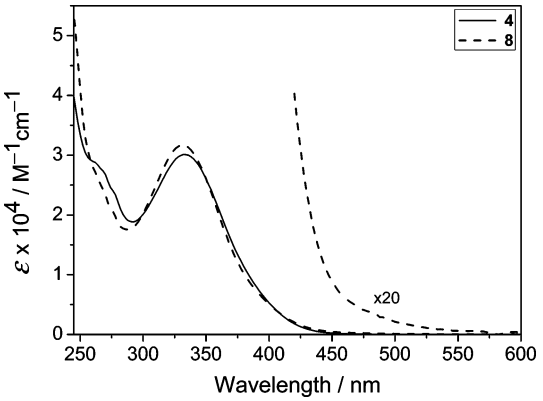

Figure 9. Electronic absorption spectra of **4** and **8** in dichloromethane at 298 K.

the intraligand transition of the phosphine ligands resulting from the presence of the phenyl groups. This is supported by the absence of such an absorption shoulder in **1** and **2**, bearing aliphatic phosphines. The band at ∼330−334 nm is suggestive of having a $^1[n(S) \rightarrow \pi^*(C_6H_4NO_2)]$ intraligand donor−acceptor-type charge-transfer character, based on the fact that such a band is also present in the absorption spectrum of the carbonimidothioate ligand and the close resemblance of the absorption energy between the ligand and all the complexes. The absorption tail beyond 420 nm for **8** is attributed to a ferrocenyl-centered absorption.

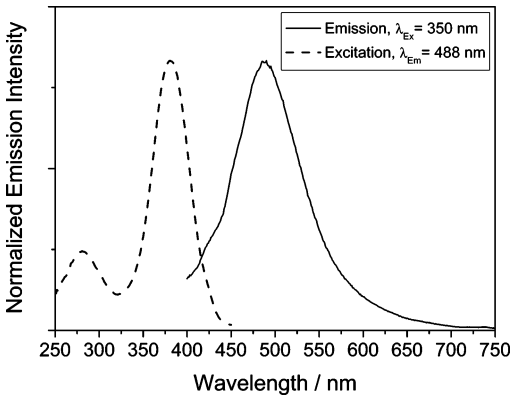

Figure 10. Emission (—) and excitation (- - -) spectra of **4** in dichloromethane at 298 K.

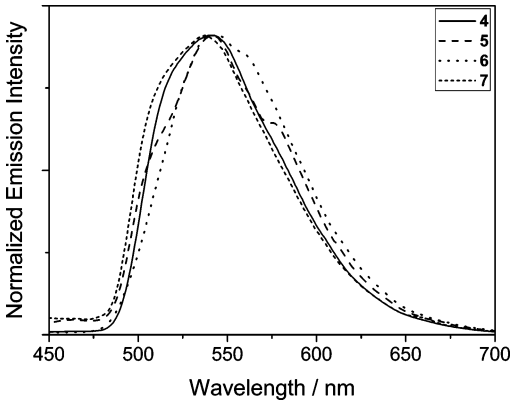

Figure 11. Solid-state emission spectra of **4**−**7** at 77 K.

Photoexcitation of complexes **1**−**7** with $\lambda > 350$ produces green and blue luminescence in the solid state and in solution, respectively. Excitation spectra recorded for the bluish-green emission in dichloromethane solutions at 298 K indicate an excitation band maximum at ∼380−387 nm. Figure 10 shows the emission and excitation spectra of **4** in dichloromethane at 298 K as a selected example. In view of the close similarity of their emission energies with respect to that observed for the ligand itself, together with the relatively long radiative lifetimes in millisecond range at 77 K, an emission origin attributed to a $^3[n(S) \rightarrow \pi^*(C_6H_4NO_2)]$ intraligand donor−acceptor charge transfer, probably mixed with some $^3[S(3p) \rightarrow Au(6s/6p)]$ ligand-to-metal charge-transfer (LMCT) character, is suggested. The observed shortening of the intraligand donor−acceptor charge-transfer phosphorescence lifetimes when the free ligand is coordinated to the gold(I) center can be rationalized as the "partial" relaxation of the forbidden triplet−singlet radiative decay by the heavy gold atom that possesses significant spin−orbit coupling. It is also noteworthy to mention that the change of the ancillary phosphines, as well as the presence or absence of Au···Au interactions, either intermolecularly or intramolecularly, do not impose significant differences on the emission energy and excitation maxima of the metal

complexes. Nevertheless, from the solid-state emission spectra of complexes **4**−**7** at 77 K (Figure 11), a subtle emission energy trend of **7** (537 nm) > **4** (541 nm) ≈ **5** (541 nm) > **6** (543 nm) is indicated, which is in line with the decrease in the short intramolecular Au···Au distances that vary from none (**7**) > 3.1589(4) Å (**4**) ≈ 3.1171(3) Å (**5**) > 3.0820(6) Å (**6**). This may be suggestive of a $^3[n(S) \rightarrow \pi^*(C_6H_4NO_2)]$ intraligand donor−acceptor charge-transfer excited-state bearing $^3[S(3p) \rightarrow Au(6s/6p)]$ LMCT character that has been modified by the weak closed-shell Au···Au interactions, albeit small. Complex **8**, on the other hand, does not show significant photoluminescence under ambient conditions. Such a phenomenon is not unusual and is attributed to the intramolecular quenching by the ferrocenyl moiety.[45]

Acknowledgment. E.R.T.T. acknowledges the support of the National University of Singapore (R-143-000-213-112). V.W.-W.Y. acknowledges support from the University Development Fund (UDF) of The University of Hong Kong and The University of Hong Kong Foundation for Educational Development and Research Limited.

Supporting Information Available: Crystallographic data (CIF) for the eight structures reported herein, as well a full listing of ^1H and ^{13}C NMR data. This material is available free of charge via the Internet at http://pubs.acs.org.

IC0608243

(45) Fery-Forgues, S.; Delavaux-Nicot, B.; Lavabre, D.; Rurack, K. *J. Photochem. Photobiol. A* **2003**, *155*, 107. (b) Thornton, N. B.; Wojtowicz, H.; Netzel, T.; Dixon, D. W. *J. Phys. Chem. B* **1998**, *102*, 2101.